Inter-brain neural mechanism underlying turn-based interaction under acute stress in women: a hyperscanning study using functional near-infrared spectroscopy

Hanxuan Zhao,[1,2] Yadan Li,[1] Xuewei Wang,[3] Yuecui Kan,[4] Sihua Xu,[2] and Haijun Duan[1]

[1]Key Laboratory of Modern Teaching Technology, Ministry of Education, Shaanxi Normal University, Xi'an 710062, China
[2]Center for Magnetic Resonance Imaging Research & Key Laboratory of Applied Brain and Cognitive Sciences, School of Business and Management, Shanghai International Studies University, Shanghai 200083, China
[3]Centre for Mental Health Education, Xidian University, Xi'an, Shaanxi 710071, China
[4]School of Psychology, Shaanxi Normal University, Xi'an 710062, China
Correspondence should be addressed to Haijun Duan, Key Laboratory of Modern Teaching Technology, Ministry of Education, Yanta Campus, Shaanxi Normal University, 199 South Chang' an Road, Xi'an 710062, China. E-mail: duanhj@126.com.

Abstract

With the ever-changing social environment, stress has exerted a substantial influence on social interaction. The present study examined the underlying cognitive and neural mechanism on how acute stress affected the real-time cooperative and competitive interaction with four hypothesized path models. We used the hyperscanning technique based on functional near-infrared spectroscopy (fNIRS) device to examine brain-to-brain coherence within the dyads engaging Pattern Game under acute stress manipulated through Trier Social Stress Test for Groups. Behavioral results showed stressed dyads exhibited better cooperative performance and higher self-other overlap level during the cooperative session than dyads in the control group. The fNIRS results identified higher interpersonal brain synchronization in the right temporal-parietal junction (r-TPJ) stronger Granger causality from partner-to-builder during the cooperative session in the stress group when compared with the control group. Our results corroborated better performance in the cooperative context and further identified that brain-to-brain coherence in r-TPJ and self-other overlap serially mediated the effect of acute stress on cooperative performance.

Key words: fNIRS; hyperscanning; acute stress; turn-based interaction; self-other overlap

Introduction

Uniquely among other species, what makes human beings extraordinary is our ability to participate in a wide range of interactions across blood ties. Social interaction is the most indispensable component of our life. As independent individuals, we interact with others in various forms every day. Interpersonal interaction occurs when the interdependent relationship is built between the intentions and manners of both sides (Deutsch, 1973). As a social relationship variable, interpersonal interaction is indispensable to promote individual mental health and subjective well-being by providing shared resources and senses of identity (Oishi, 2000; Cohen, 2004; Zhang *et al.*, 2016). However, with the ever-changing social environment, stress has become an inevitable lifestyle that everyone is facing. When facing stress, the synergistic activation of sympathetic-adrenal-medullary (SAM) and hypothalamic-pituitary-adrenal (HPA) axis

may cause habitual emotional response bias during social interaction (Ulrich-Lai and Herman, 2009). Hence, uncovering human response patterns in the social context under stress and its underlying neural mechanism is of far-reaching significance.

Prior studies have made an intriguing discussion regarding individuals' response patterns under stress in the social context with the single-brain approach. On the one hand, some studies focusing on the effect of stress on social behavior argued that stress might enhance the arousal level to prepare for adaptive behavioral responses to stressors. This kind of response pattern is referred to as 'fight-or-flight' response (Cannon, 1939). The 'fight-or-flight' response pattern claimed that individuals under stress exhibit higher aggressiveness and vigilance during social interaction and pay more attention to self-interest (Steinbeis *et al.*, 2015). A biobehavioral study reported that acute stress damaged social memory that is indispensable in interpersonal cooperation

(Takahashi, 2005). It is also reported that the stressed individuals exhibited less trust and altruistic punishment (Steinbeis *et al.*, 2015). Another study using the Everyday Moral Decision-Making paradigm investigated how acute stress affects moral decision-making, demonstrating that cortisol response was negatively correlated with altruistic decisions in emotional dilemmas (Starcke *et al.*, 2011). On the other hand, another strand of studies also argued that individuals under stress might show the 'tend-and-befriend' response pattern by affiliating with social groups to gain more support to face the stressful environments (Von Dawans *et al.*, 2012). The 'tend-and-befriend' response pattern originally delineated females' coping mechanisms under acute stress and then extended to men (Taylor, 2006; Von Dawans *et al.*, 2012). Evidence for the 'tend-and-befriend' hypothesis has also been accumulated. Prior studies using different paradigms to examine individuals' prosocial and nonsocial behavior have manifested prosocial inclination under acute stress in both males and females (Von Dawans *et al.*, 2012, 2019). Evidence also showed that acute stress enhanced emotional empathy assessed by the multifaceted empathy test (Wolf *et al.*, 2015). The 'tend-and-befriend' response pattern has also been corroborated in the dictator game (Tomova *et al.*, 2016). Nevertheless, the 'tend-and-befriend' response and 'fight-or-flight' individuals' response patterns in the social context under acute stress in the existing literature were simply examined with the single-brain approach due to the limited techniques. The nature of continuity and dynamics in the interactive context has been largely neglected.

With the emerging dual-brain approach, some recent advance has shed some light on the effect of stress on social interaction in the real-time interactive context, and the existing evidence concerning the issue still presents a complex and inconsistent picture. On the one hand, some studies verified better cooperative performance and enhanced within-group synchronization under the pressure. A recent study adopting the newly-developed intergroup aggressor-defender conflict game examined the effect of out-group conflict pressure on the in-group defense and further demonstrated better in-group cooperation and coordination when facing out-group threat and pressure (De Dreu *et al.*, 2016). Recent neurophysiological evidence investigating the effect of oxytocin on in-group coordination under the inter-group conflict in a real-time economic game further manifested the promoting effect of the oxytocin on the interpersonal coordination under the out-group pressure (Zhang *et al.*, 2019). The most representative study using the functional near-infrared spectroscopy (fNIRS)-based hyperscanning technique also verified the increased within-group synchronization in both the r-DLPFC and the right temporal-parietal junction (r-TPJ) under the pressure of out-group attack, and reported a positive correlation between the within-group brain synchronization and the intergroup hostility (Yang *et al.*, 2020). On the other hand, recent advances also reported the promoting effect on both cooperative and competitive performance under acute stress on the behavioral and neural levels. A recent fNIRS-based hyperscanning study adopting the Montreal Imaging Stress Task (MIST) which induced relatively a low-intensity stress state also reported the facilitating effect of acute stress on both concurrent competition and cooperation which were a relatively rare interactive mode in real life, and further reported the enhanced concomitant inter-brain synchronization during the concurrent competition and cooperation under acute stress (Zhang *et al.*, 2021). The aforementioned inconsistency in the prior literature might be contributed to the following two aspects. On the one hand, the existing evidence

only adopted the relatively low-intensity stress induction methods, and no physiological parameters were detected when inducing the out-group pressure. On the other hand, prior literature adopting different social interaction paradigms simply mixed different dimensions of interpersonal interaction or omitted the interdependence between group members. Based on the existing advances, the present study examined the effect of acute stress induced by the robust Trier Social Stress Test (TSST) on turn-based interaction which has been considered as the core process of social interaction (Pickering and Garrod, 2013; Zheng *et al.*, 2020).

Although the existing evidence has preliminarily uncovered the effect of stress on interpersonal interaction, the potential cognitive and neural mechanisms and its internal relationship underlying social interaction under acute stress still need to be identified. On the one hand, recent neurohormonal evidence has revealed the potential association between the hormonal changes induced by stress and self-other connectedness during social interaction. The positive correlation between cortisol responses and in-group social bonding was reported in both men and women (Berger *et al.*, 2016; Schweda *et al.*, 2019; Von Dawans *et al.*, 2019). On the other hand, the putative mechanism addressing that brain-to-brain synchronization could be an epiphenomenon of social connectedness in a shared social environment during social interaction has been supported by some latest advances (Hasson *et al.*, 2012; Gvirts and Perlmutter, 2020; Valencia and Froese, 2020). An fNIRS-based hyperscanning study reported that interpersonal brain synchronization predicted mutual prosociality (Hu *et al.*, 2017). The parent–child inter-brain coupling also mediated the relationship between parents' and child's emotional regulation (Reindl *et al.*, 2018). Taken together with prior cognitive and neural evidence, recent neuroimaging studies also reported the association between brain-to-brain coherence and self-other connectedness. A wireless-EEG-based hyperscanning study investigating real-world learning reported a positive correlation between perceived closeness and brain-to-brain coupling (Bevilacqua *et al.*, 2019). The increased interpersonal brain synchronization was also correlated with behavioral cooperative performance (Xue *et al.*, 2018), and this correlation was also verified among the dyads in romantic relationships (Pan *et al.*, 2017; Duan *et al.*, 2022). Self-reported shared intentionality, perceived similarity, perspective-taking and empathy are also associated with the detected brain-to-brain coherence (Hu *et al.*, 2017; Liu *et al.*, 2017). The latest fNIRS-based hyperscanning study firstly provided direct evidence for the potential cognitive and neural mechanisms underlying prosocial behavior, demonstrating that self-other overlap level and inter-brain coherence played a serial mediating role in how behavioral synchronization affected prosocial behaviors (Feng *et al.*, 2020). Hence, the present study intends to investigate the cognitive and neural underpinnings concerning how acute stress affects turn-taking interaction using self-other connectedness and inter-brain synchronization as the proposed mediators.

With the emerging hyperscanning technique, the inter-brain coupling during the social interaction has been verified in the brain regions in the mirror neuron system (MNS) and mentalizing system (MS). The MNS covering the inferior parietal lobule (IPL), inferior frontal gyrus (IFG) and superior temporal gyrus (STG) has been regarded as a crucial neural system for action understanding (Wang *et al.*, 2018). The MNS can identify and simulate the aim of the action by matching the perceived action information with the existing action experience (Keysers and Gazzola, 2007; Van Overwalle and Baetens, 2009). Recent hyperscanning studies reported
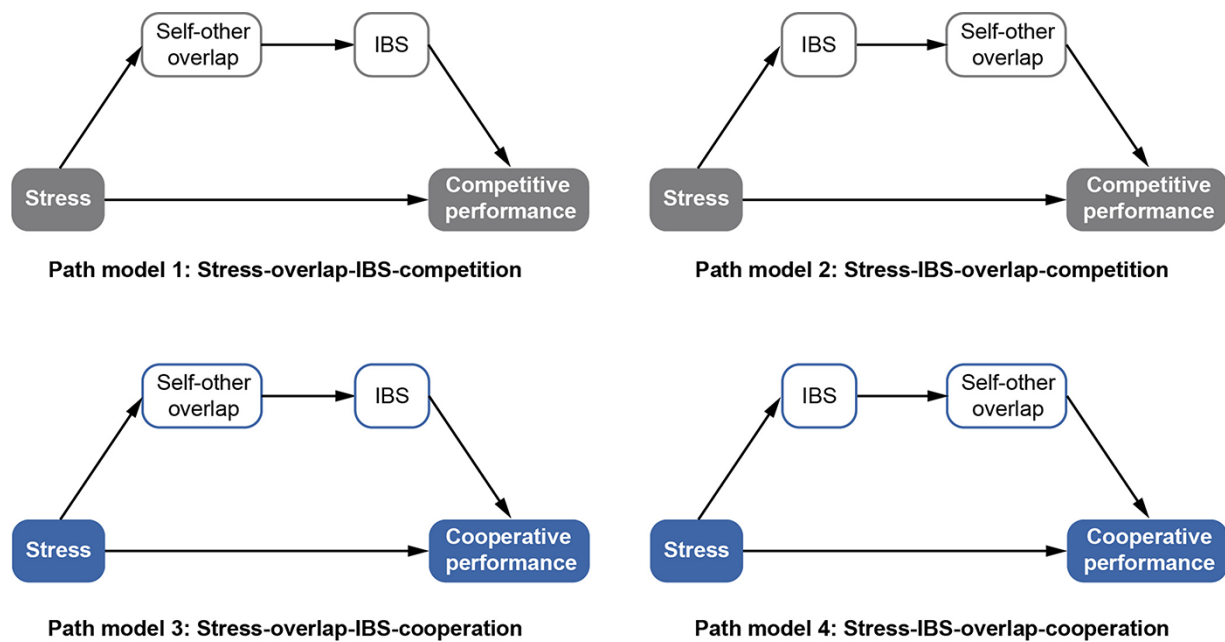
Fig. 1. Four conceptual path models of the hypothesized mechanism.

the brain-to-brain coupling in the MNS during interpersonal coordination and imitation (Dumas *et al.*, 2010; Ménoret *et al.*, 2014). The MS covering the medial prefrontal cortex (mPFC) and the temporo-parietal junction (TPJ) covering angular gyrus (AG) and supramarginal gyrus (SMG) can decode others' intention and encode the mental representation to achieve information exchange (Amodio and Frith, 2006; Wang *et al.*, 2018). It is known that the dorsomedial prefrontal cortex (dmPFC) was involved during the self-other representation on the cognitive level, and the ventromedial prefrontal cortex (vmPFC) was involved during the self-other closeness on the affective level (Lieberman *et al.*, 2019; Courtney and Meyer, 2020). Substantial neuroimaging evidence has also reported the essential role that r-TPJ has played in the self-other representation. It is well-documented that the r-TPJ was recruited in self-awareness (Salgues *et al.*, 2021), self-other distinction (Eddy, 2016), perspective-taking (Blakemore and Frith, 2003; Decety and Lamm, 2007) and theory of mind (Igelström *et al.*, 2016). Numerous hyperscanning studies have also reported the inter-brain coherence in the TPJ during the social interaction involving the self-other representation which covered the face-to-face communication (Jiang *et al.*, 2012), cooperation (Cui *et al.*, 2012), competition (Liu *et al.*, 2015), interactive learning (Pan, Guyon, *et al.*, 2020) and economic exchange (Tang *et al.*, 2016). Prior fNIRS-based hyperscanning study has addressed that the inter-brain coherence in the right hemisphere was induced by non-verbal communication, and the inter-brain coherence in the left hemisphere was induced by verbal communication (Osaka *et al.*, 2014). Since no verbal communication was allowed when the dyad completed the pattern game in the present study, the right fronto-tempo-parietal region covering most of the main region in the MNS and MS has been chosen as the region of interest in the present study. It should be noted that the right mPFC was not taken into account due to the limited spatial resolution of fNIRS devices (Pinti *et al.*, 2020).

To sum up, the present study intends to elucidate the cognitive and neural mechanism of the response pattern under acute stress in the real-time cooperative and competitive interactive context with the dual-brain approach by using the fNIRS-based hyperscanning technique. The underlying mechanism of the interpersonal interaction under acute stress has been examined by integrating the related parameters on the biochemical-psychological-brain level, and the evidence of the temporal chain effect has been further verified by examining the four rival path models, respectively (see Figure 1). The stress condition was manipulated with TSST-G, and the corresponding physiological and psychological indicators were collected to verify the successful induction. The cooperative and competitive performance was assessed using Pattern Game adapted by Liu *et al.* (Liu *et al.*, 2015). In line with prior research, social connectedness during the interaction was assessed by the Inclusion of the Other in the Self (IOS) Scale (Aron *et al.*, 1992; Feng *et al.*, 2020). Brain-to-brain activities were simultaneously measured with the fNIRS hyperscanning technique.

Based on the prior advances, our hypotheses were delineated as follows:

H1: Different behavioral patterns under acute stress would exhibit in the competitive and cooperative context.

H2: Increased inter-brain synchronization in the r-TPJ would be identified due to better interactive performance of the stressed dyads.

H3: Given that social connectedness may be the potential cognitive mechanism in social interaction, the positive correlation between increased inter-brain coherence and self-other overlap would also be identified.

H4: Based on the prior neurobiological model proposed by Gvirts & Perlmutter, at least one of the four hypothesized path models would be verified.

Methods
Participants

Prior to the formal experiment, a statistical power analysis was performed for the sample size estimation using G*POWER 3.1.9.7 statistical analysis program (Faul *et al.*, 2007). With Type I error
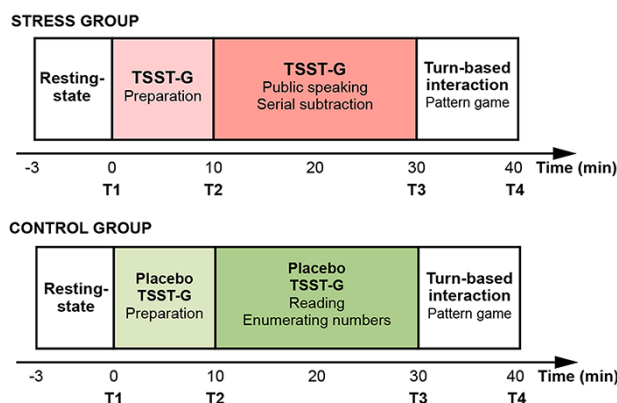
STRESS GROUP

| Resting-state | TSST-G Preparation | TSST-G Public speaking Serial subtraction | Turn-based interaction Pattern game |

-3   0   10   20   30   40   Time (min)
T1   T2   T3   T4

CONTROL GROUP

| Resting-state | Placebo TSST-G Preparation | Placebo TSST-G Reading Enumerating numbers | Turn-based interaction Pattern game |

-3   0   10   20   30   40   Time (min)
T1   T2   T3   T4

Fig. 2. Experimental protocol. (A) Overall experimental timeline.

of 0.05 ($\alpha = 0.05$) and Type II error of 0.05 ($1—\beta = 0.95$), the projected total sample size was 44 with the expected effect size of 0.25 (Cohen's $f = 0.25$) based on our experimental design (Cohen, 2013). Hence, 88 healthy, right-handed females with a mean age of 20.13 years (s.d. = 1.21 years) forming 44 dyads were recruited in the present study. Each participant was randomly paired with another stranger partner. All dyads were randomly assigned to either the stress group ($N = 22$) or the control group ($N = 22$). Due to the potential gender difference in the stress response and the existing gender composition effect reported by prior studies (Youssef *et al.*, 2012; Lu *et al.*, 2020a), we recruited female students to avoid the effect of the extraneous variables. All participants were prescreened by Trait Anxiety Inventory (T-AI) and Beck Depression Inventory (BDI-II) (Booij *et al.*, 2015; Kan *et al.*, 2019). Consistent with the prior studies, only participants within 0–13 BDI-II scores and 35–50 T-AI scores were recruited (Smarr and Keefer, 2011; Kan *et al.*, 2019). The averaged T-AI score (mean = 41.43, s.d. = 4.56) and the averaged BDI-II score (mean = 4.33, s.d. = 3.53) of the recruited participants were all in the normal range. Endogenous-cortisol-concentration-related exclusionary criteria covered prior participation of the acute stress induction task, drug abuse, alcohol or caffeine intake, the use of hormonal contraceptives, acute or chronic disease and menstruation (Shields *et al.*, 2016). The range of the Body Mass Index (BMI) was from $18\,kg/m^2$ to $27\,kg/m^2$. The strenuous exercises, dining and drinking (including water) 3 h before the experiment were forbidden. All participants signed informed consent. Our research has complied with the Declaration of Helsinki. Our study was approved by the Academic Committee of Key Laboratory of Modern Teaching Technology, Ministry of Education, Shaanxi Normal University in China.

Tasks and procedures

The experiments were conducted between 14:00 and 18:00 based on the diurnal fluctuation of cortisol level (Izawa *et al.*, 2010). When participants arrived at the laboratory, they filled in the demographic information. Each dyad sat side-by-side in front of one computer screen. After the brief acquaintance, the experimenter of the present study introduced the whole experimental procedure and asked them to finish the practice experiment to affirm that they fully understood the requirements of the task.

The formal experimental protocol consisted of a 3-min-resting-state session, a 30-min-stress (or placebo)-inducing session and a 10-min-turn-based interaction session (Figure 2).

The 3-min-resting-state session served as a baseline for further analysis. The experimental tasks in the other two sessions were delineated below. Salivary cortisol and Positive and Negative Affect Schedule (PANAS) scores were used as physiological and psychological indicators of acute stress induction (Kan *et al.*, 2019). The experimenter collected salivary samples and affective data on PANAS after the resting-state session (T1), the preparation phase in TSST-G (Placebo TSST-G) task (T2), TSST-G (Placebo TSST-G) task (T3) and turn-based interaction session (T4). The pre-experiment and post-experiment questionnaires were also described as follows. The timeline has been shown in Figure 2.

Acute stress induction

The present study adopted the TSST-G to manipulate acute stress state (Von Dawans *et al.*, 2011). The between-participant experimental design was used in the manipulation of the induction of acute stress state. The dyads in the stress group completed TSST-G, while the dyads in the control group performed corresponding placebo TSST-G.

The TSST-G experimental procedure consisted of three sessions. Firstly, participants were first given 10 min to prepare. Each participant was then asked to give a 5-min self-introduction speech during a mock job interview. The interview panel consisted of two whited-coated experimenters. Digital videos situated in front of the participant recorded the whole interview. Dyads were then required to complete a serial subtraction task. Once a mistake was made, the participant would be required to start all over again from the starting number.

The placebo TSST-G task was designed in the same manner without the exposition to any stressful components. After the preparation, participants were asked to read the scientific text in a low voice. Participants were then asked to enumerate a series of numbers in a low voice. Neither interview panel in white coats nor digital videos was present when participants performed the task.

Pattern game

The current study adopted a turn-based interactive pattern game adapted by Liu *et al.* (Liu *et al.*, 2015). Each dyad of participants sitting side-by-side played pattern game in a turn-based manner under two experimental conditions (cooperation and competition conditions) and one control condition (independent condition) without any verbal communication. Two participants in a dyad

were randomly assigned to different roles in the game. The one assigned as a BUILDER was instructed to duplicate the target pattern by consistently controlling YELLOW disks. The other one assigned as a PARTNER was instructed to either help (in cooperation condition) or obstruct (in competition condition) the builder's progress by consistently controlling BLUE disks. Participants were required to duplicate the pattern independently under the other participant's watching in an independent condition. In line with prior research, the entire experiment consisted of 14 sessions: four cooperation sessions, four competition sessions, four independent sessions and two rest sessions (Liu *et al.*, 2015). The presentation sequence of sessions was pseudo-randomized. Other details in the experimental session aligned with the prior research (Liu *et al.*, 2015).

A 5 × 5 grid game board and a target pattern made of five tokens within a 3 × 3 matrix were displayed on the screen. The yellow or blue disk appeared automatically on the game board's left-top side, designating it was whose turn to play. Each dyad of participants chose the aimed column by controlling the disk's horizontal displacements via the keys on the keyboard, and the disk dropped instantly to the lowest available slot in the targeted column. Each dyad was given 2 s for moving the disk in each turn. Other experimental details were aligned with prior research (Liu *et al.*, 2015). Before the formal experiment, each dyad of participants obtained coaching on the above three types of conditions until the dyad completely comprehended the game and played the game without mistakes.

Post-experimental questionnaires

In line with prior research, we adopted the IOS scale to assess the degree of self-other overlap and the feelings of social connectedness in the experiment (Aron *et al.*, 1992). The IOS scale is a reliable single-item, pictural tool assessing the level of psychological overlap between the other and the self (Aron *et al.*, 1997). After completing the experiment, participants were required to evaluate the extent to which they and their partners connected in the cooperation condition, competition condition and independent condition. Higher scores represented a higher level of social connectedness. No communication within the dyad was permitted while rating.

Data acquisition
Stress-related data acquisition

Following our prior studies, the validation of acute stress induction was verified by both physiological and psychological indicators in the present study (Kan *et al.*, 2019; Duan *et al.*, 2020). Physiological indicators included the salivary cortisol and the heart rate. The saliva samples were collected by Salivettes® (Sarstedt 51.1534.500, Germany), and the salivary cortisol in saliva samples was analyzed by the enzyme-linked immunosorbent assay (ELISA) method. The heart rate was collected by BIOPAC MP150 system (BIOPAC Systems, Goleta, CA), and the average heart rate was calculated by the AcqKnowledge 5.0 software.

Psychological indicators included the positive affect scores and the negative affect scores assessed by PANAS. The time points of the collection of saliva samples and PANAS scores were manifested in Figure 2.

fNIRS data acquisition

An fNIRS system with 38 channels (LABNIRS; Shimadzu Co., Japan) was adopted to simultaneously record dyads' cerebral

activities. The relative oxyhemoglobin (HbO) and deoxyhemoglobin (HbR) concentrations were converted using modified Beer–Lambert law (Pellicer and del Carmen Bravo, 2011). The sampling rate for measurement was 10 Hz. Due to the higher signal-to-noise rate and greater sensitivity of HbO concentration in the cerebral blood flow, the present research only focused on HbO concentration (Hoshi, 2003; Lindenberger *et al.*, 2009; Cui *et al.*, 2012; Mahmoudzadeh *et al.*, 2013). The region of interest in the current study was the right fronto-tempo-parietal region, which was recruited in social interaction (Liu *et al.*, 2015; Wang *et al.*, 2018).

As presented in Figure 3A, a 3 × 5 optode probe patch was placed on each participant's right fronto-tempo-parietal region covering IFG, STG, angular gyrus (AG) and IPL (8 emitters and 7 detectors, 22 channels, 30 mm optode separation). The placement was consistent with international 10–20 system. The bottom line of probe patch aligned with sagittal reference curve. The reference optode was located at P6. We used a 3D magnetic space digitizer (FASTRAK; Polhemus, USA) to assess anatomical positions of optodes and channels (CHs) with NZ, CZ, AL, AR as referential points. The spatial anatomical location was further analyzed by the NIRS_SPM MATLAB package. The BrainNet Viewer was adapted in the visualization of the channels (Xia *et al.*, 2013).

Data analysis
Physiological data analysis

To examine whether the acute stress induction was valid, the area under the curve with respect to the increase (AUC_I) across four salivary samples (T1–T4) was calculated. The AUC_I has been considered a reliable index that can better reflect the physiological changes over time and neglect the individual responsivity (Pruessner *et al.*, 2003). With reference to prior studies, the AUC_I was defined below (Pruessner *et al.*, 2003).

$$AUC_I = \left(\sum_{i=1}^{n-1} \frac{\left(m_{(i+1)} + m_i\right) \cdot t_i}{2} \right) - \left(m_1 \cdot \sum_{i=1}^{n-1} t_i \right)$$

In the formula above, *m, t, n,* respectively represent the salivary cortisol in one measurement, the time distance among measurements and the total amount of measurements.

Behavioral data analysis

We adopted mean error rate (%) to measure participants' behavioral performance (Decety *et al.*, 2004; Liu *et al.*, 2015, 2017). Aligning with prior studies, an error was documented if the BUILDER made one move against the target pattern or the PARTNER made one move disrupted (in cooperation condition) or helped (in competition condition) the BUILDER (Liu *et al.*, 2015).

fNIRS data analysis
Preprocessing. The quality of fNIRS data was examined by checking if a distinct heart frequency band around 1 Hz was acquired in the wavelet transform plot (Lu *et al.*, 2020b; Zhao *et al.*, 2021). The channels exhibiting poor signals were displaced by averaging fNIRS signals in the adjacent channels, and the fNIRS data of the dyad were excluded from further analysis when more than half of the channels exhibited bad signals (Lu *et al.*, 2020b). Since no dyad exhibited bad signals in more than half of the channels, the fNIRS data of all 44 dyads were involved in the present study. Each dyad's data were preprocessed using NIRS_SPM
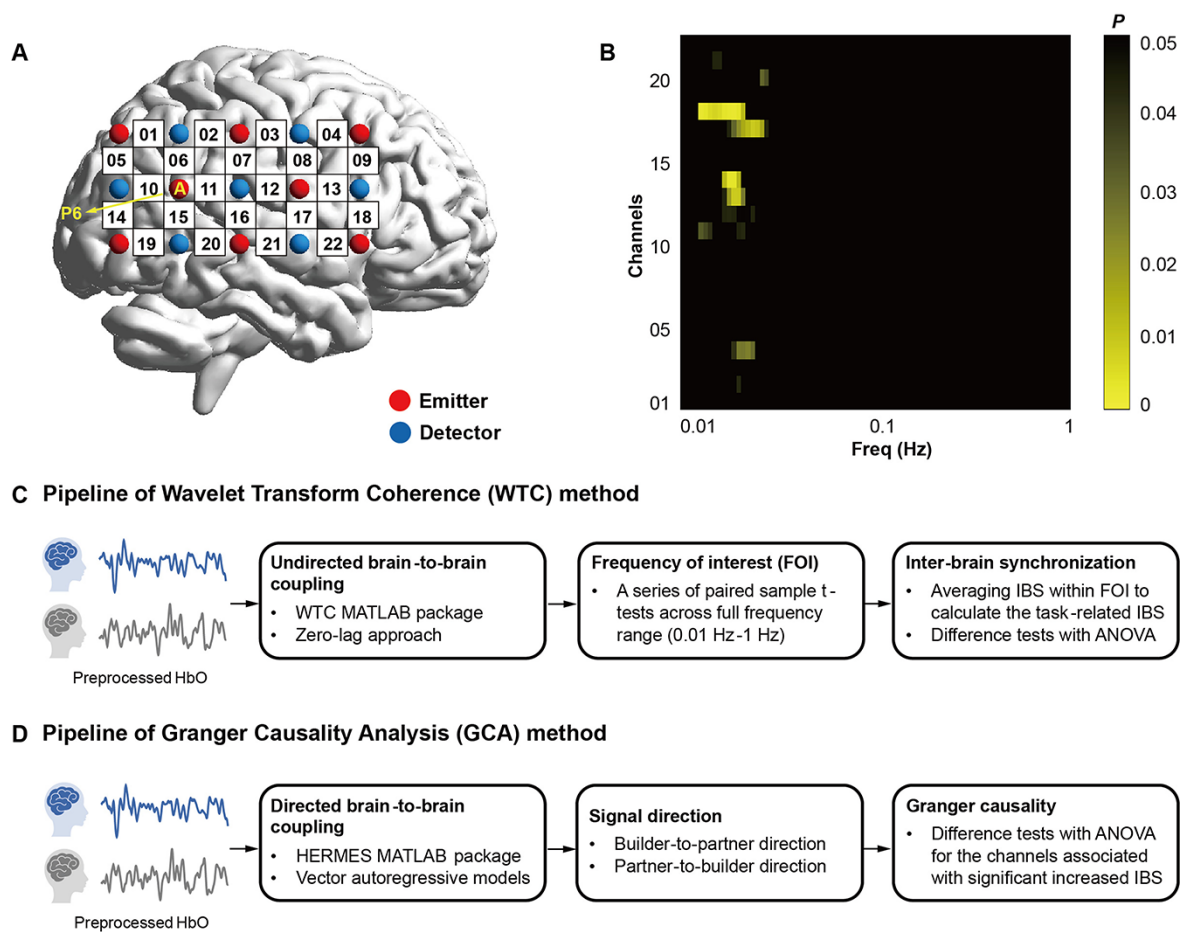
Fig. 3. (A) Optode probe configuration; (B) FDR-corrected *p*-maps when comparing the IBS during the turn-based interaction session with the IBS during the resting-state session across full frequency range (0.01 Hz–1 Hz); (C) Pipeline of Wavelet Transform Coherence (WTC) method; (D) Pipeline of Granger Causality Analysis (GCA) method.

MATLAB package with hemodynamic response function (HRF) low-pass filtering which could correct the temporal autocorrelation in NIRS data, and Wavelet-MDL detrending algorithm which could remove unknown global trends caused by motion noises, breathing, cardiac or other artifacts. (Ye *et al.*, 2009).

Interpersonal brain synchronization (IBS). The preprocessed data were analyzed using the wavelet transform coherence (WTC) MATLAB package aiming at examining the relationship between the fNIRS time signals of the participants (Grinsted *et al.*, 2004). Aligning with existing studies examining the turn-based interaction with the WTC method (Zhang *et al.*, 2017; Lu *et al.*, 2018, 2020b), the zero-lag approach in the WTC method was adopted when calculating the brain-to-brain coupling within the BUILDER-to-PARTNER dyads to avoid possible biases that might be induced by the slow cerebral blood flow response and the current experimental design (Schroeter *et al.*, 2006). The validity of the zero-lag approach has also been verified by the prior study using the same experimental paradigm (Liu *et al.*, 2015). The WTC of fNIRS signals $i(n)$ and $j(n)$ was denoted below (Grinsted *et al.*, 2004; Nozawa *et al.*, 2016).

$$\text{WTC}(n,s) = \frac{\left|\langle s^{-1} W^{ij}(n,s) \rangle\right|^2}{\left|\langle s^{-1} W^{i}(n,s) \rangle\right|^2 \left|\langle s^{-1} W^{j}(n,s) \rangle\right|^2}$$

To identify the frequency of interest (FOI), we compared the IBS during the turn-based interaction session with the IBS during the resting-state session across full frequency range (0.01 Hz–1 Hz) (Nozawa *et al.*, 2016; Pan, Dikker *et al.*, 2021). Before comparing the IBS during the task session and the resting-state session, the averaged IBS was converted using the Fisher z transformation (Chang and Glover, 2010; Cui *et al.*, 2012). We used a series of paired sample *t*-tests to estimate whether averaged IBS during turn-based interaction sessions was significantly higher than the averaged IBS during the resting-state session. The *P*-values were further corrected with the false discovery rate (FDR) correction method. Results found that IBS during the task session was significantly higher than the IBS during the resting-state session within the frequency band ranging from 0.012–0.025 Hz (FDR-corrected *P* < 0.05, see Figure 3B). Therefore, the frequency band was selected as the frequency band of interest (FOI) in the present study. The FOI aligned with prior fMRI studies addressing that the low-frequency oscillations ranging from 0.01 Hz to 0.1 Hz were more reliable markers of neural synchronization than the high-frequency oscillations (Achard *et al.*, 2006; Zuo *et al.*, 2010; Xue *et al.*, 2018), and also excluded low-frequency fluctuations below 0.01 Hz and the physiological noises related to Mayer waves (0.1 Hz), respiration (0.2–0.3 Hz) and cardiac pulsation (0.7–4 Hz) (Guijt *et al.*, 2007; Tong *et al.*, 2011; Nozawa *et al.*, 2016).

In line with prior studies, we further averaged the IBS within FOI across all conditions and all channels (Pan, Dikker *et al.*, 2021). We calculated the index of task-related IBS by subtracting the IBS in the resting-state session from the IBS in the turn-based interaction session, which was denoted below.

$$IBS_{task-related} = IBS_{task} - IBS_{resting-state}$$

The task-related IBS was further converted using the Fisher z transformation (Pan, Dikker *et al.*, 2021). A series of mixed-design ANOVAs using GROUP (stress, control) as a between-participant factor and CONDITION (competition, cooperation, independent) as a within-participant factor were then conducted on tasked-related IBS of all channels. The yielded *P*-values were further corrected using FDR correction method. The BrainNet Viewer was used to visualize the *F*-maps on the brain (Xia *et al.*, 2013). The pipeline of the WTC method has been illustrated in Figure 3C.

Coupling directionality. Granger causality analysis (GCA) has been widely adopted in the existing fNIRS-based hyperscanning studies. In the present study, GCA was conducted on the HbO time series in the channels exhibiting significant task-related IBS to further examine the directionality of inter-brain synchronization following the prior fNIRS-based hyperscanning studies (Zhang *et al.*, 2017; Chen *et al.*, 2020; Duan *et al.*, 2022; Pan, Guyon, *et al.*, 2020). GCA has been regarded as a reliable method to estimate the directionality between fNIRS time series within each dyad using vector autoregressive models (Granger, 1969; Chen *et al.*, 2020). With reference to the existing literature, the univariate autoregressive models of fNIRS signals *x* (*t*) and *y* (*t*) were, respectively denoted below.

$$x(t) = \sum_{k=1}^{p} a_k x_{(t-k)} + \varepsilon_x$$

$$y(t) = \sum_{k=1}^{p} a'_k y_{(t-k)} + \varepsilon_y$$

Based on the univariate autoregressive models above, the variables *y* (*t*) and *x* (*t*) were, respectively added to the models, and the bivariate autoregressive models of fNIRS signals *x* (*t*) and *y* (*t*) were, respectively denoted below.

$$x(t) = \sum_{k=1}^{p} a_k x_{(t-k)} + \sum_{k=1}^{p} b_k y_{(t-k)} + \varepsilon'_{xy}$$

$$y(t) = \sum_{k=1}^{p} a'_k y_{(t-k)} + \sum_{k=1}^{p} b'_k x_{(t-k)} + \varepsilon_{xy}$$

The variances of the residuals in the aforementioned univariate and bivariate autoregressive models were calculated by GCA, and the Granger causality on the directions of $x(t) \rightarrow y(t)$ and $y(t) \rightarrow x(t)$ was, respectively denoted below.

$$GC_{x \rightarrow y} = \ln \frac{var(\varepsilon_y)}{var(\varepsilon_{xy})}$$

$$GC_{y \rightarrow x} = \ln \frac{var(\varepsilon_x)}{var(\varepsilon_{xy})}$$

In the formulas above, $GC_{x \rightarrow y}$ represents the directed Granger causality from *x* (*t*) to *y* (*t*), and $GC_{y \rightarrow x}$ represents the directed Granger causality from *y* (*t*) to *x* (*t*).

We used the HERMES MATLAB package to compute Granger causalities in both builder-to-partner direction and partner-to-builder direction (Zhang *et al.*, 2017). Aligning with the WTC analysis in the present study, no time delay between the BUILDER and PARTNER (zero-lag approach) was considered in the GCA analysis. At last, a mixed-design ANOVA with GROUP (stress and control) as a between-participant factor, CONDITION (cooperation, competition and independent) and DIRECTION (builder-to-partner and partner-to-builder) as within-participant factors were conducted to examine the difference between the two directions under different conditions. The BrainNet Viewer was used to visualize the coupling directionality on the brain (Xia *et al.*, 2013). The pipeline of the WTC method has been illustrated in Figure 3D.

Serial mediation effect analysis
The present study evaluated the hypothesized path models using the software MPLUS 8.0. The statistical significance of the mediating effect was examined using the 95% bias-corrected confidence interval (CI) based on 1000 bootstrapping samples. If bootstrapped 95% CI did not contain zero, the mediating effects were regarded as significant at 0.05 level (Feng *et al.*, 2020). The evaluation of the hypothesized models was on the basis of the following fixed statistics: Chi-Square Test (χ^2), Root Mean Square Error of Approximation (RMSEA), Standardized Root Mean Square Residual (SRMR), Comparative Fit Index (CFI) and Tucker-Lewis Index (TLI).

Results
Validity of acute stress induction
Physiological parameters

A mixed-design ANOVA with GROUP (stress and control) as between-participant factor and TIME (T1, T2, T3 and T4) as a within-participant factor was conducted on the collected salivary cortisol. Results showed the significant main effects of TIME, $F(3, 258) = 96.97$, $P < 0.001$, $\eta_p^2 = 0.53$, and GROUP, $F(1, 86) = 158.13$, $P < 0.001$, $\eta_p^2 = 0.65$. The significant interaction effect of TIME × GROUP was also observed, $F(3, 258) = 57.82$, $P < 0.001$, $\eta_p^2 = 0.40$. Following simple effect analysis found that salivary cortisol levels in the stress group were significantly higher than that in the control group at T2 ($P < 0.001$), T3 ($P < 0.001$) and T4 ($P < 0.001$).

Using the formula mentioned above, we also applied an independent sample *t*-test on calculated AUC_I of collected salivary cortisol. Results also manifested that the AUC_I in stress group was significantly higher than AUC_I in the control group, $t(86) = 8.54$, $P < 0.001$.

A mixed-design ANOVA with GROUP (stress and control) as between-participant factor and TIME (T1, T2, T3 and T4) as a within-participant factor was conducted on the collected heart rate. Results showed the significant main effects of TIME, $F(3, 258) = 116.80$, $P < 0.001$, $\eta_p^2 = 0.57$, and GROUP, $F(1, 86) = 14.89$, $P < 0.001$, $\eta_p^2 = 0.15$. The significant interaction effect of TIME × GROUP was also observed, $F(3, 258) = 68.865$, $P < 0.001$, $\eta_p^2 = 0.45$. Following simple effect analysis found that the heart rate in the stress group was significantly higher than that in the control group at T2 ($P < 0.01$), T3 ($P < 0.001$) and T4 ($P < 0.05$). The variation trend of the heart rate during the whole experiment has been depicted in Figure 4B.
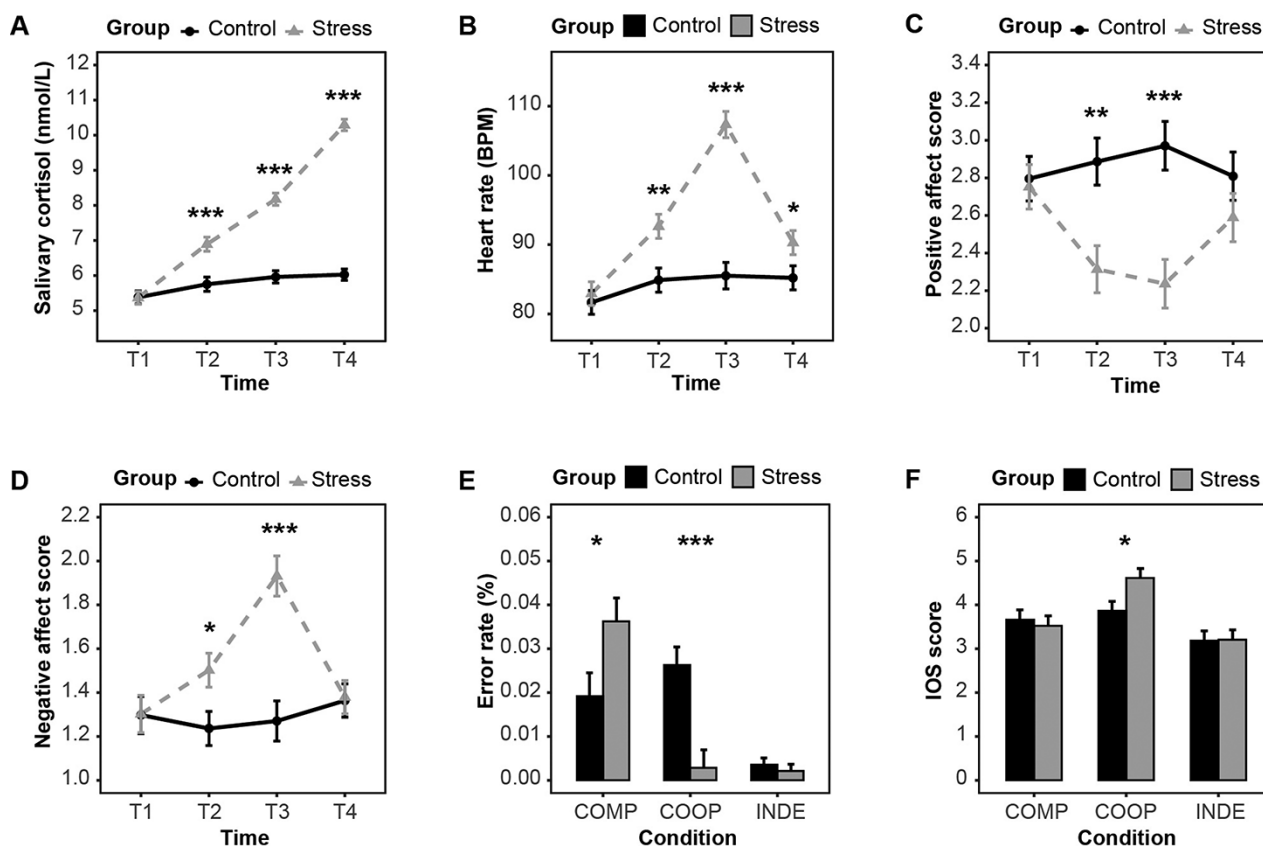
Fig. 4. Physiological and behavioral performance. (A) The salivary cortisol in stress and control groups; (B) The heart rate in stress and control groups; (C) The positive affect score in stress and control groups; (D) The negative affect scores in stress and control groups; (E) The error rate of stress and control groups in pattern game; (F) The self-other overlap level in stress and control group. Error bars represent standard errors of mean. * P <0.05, ** P <0.01, *** P <0.001.

Psychological parameters

A mixed-design ANOVA with GROUP (stress and control) as between-participant factor and TIME (T1, T2, T3 and T4) as a within-participant factor was, respectively conducted on positive affect scores and negative affect scores in PANAS. Results regarding positive affect scores manifested a significant main effect of GROUP, $F(1, 86) = 10.96$, $P < 0.01$, $\eta_p^2 = 0.11$. A significant interaction effect of TIME × GROUP was also observed, $F(3, 258) = 4.33$, $P < 0.01$, $\eta_p^2 = 0.05$. Subsequent simple effect analysis further manifested that positive affect score in the stress group was significantly lower than that in the control group at T2 ($P < 0.01$) and T3 ($P < 0.001$).

Results regarding the negative affect score manifested the significant main effects of TIME, $F(3, 258) = 9.18$, $P < 0.001$, $\eta_p^2 = 0.10$, and GROUP, $F(1, 86) = 6.96$, $P < 0.01$, $\eta_p^2 = 0.08$. The significant interaction effect of TIME × GROUP was also observed, $F(3, 258) = 12.59$, $P < 0.001$, $\eta_p^2 = 0.13$. The subsequent simple effect analysis showed that the negative affect score in the stress group was significantly higher than that in the control group at T2 ($P < 0.05$), and T3 ($P < 0.001$).

Behavioral performance in turn-based interaction

As mentioned above, the error rate during the pattern game in both the stress and control groups was calculated. In line with the prior studies, all participants' error rates in all conditions were less than 5%, corroborating that all participants have understood instructions and completed the game effectively. To further identify performative differences among all conditions in both groups, a mixed-design ANOVA using GROUP (stress and control) as between-participant factor and CONDITION (competition, cooperation and independent) as a within-participant factor was employed on error rate during the pattern game. Results found a significant main effect of CONDITION, $F(2, 172) = 19.80$, $P < 0.001$, $\eta_p^2 = 0.19$. A significant interaction effect of CONDITION × GROUP was also observed, $F(2, 172) = 12.69$, $P < 0.001$, $\eta_p^2 = 0.13$. The following simple effect analysis showed that the error rate of the stress group was significantly higher than that of the control group in the competition session ($P < 0.05$), while the error rate of the stress group was significantly lower than that of the control group in cooperation session ($P < 0.001$). The results above were depicted in Figure 4.

Subjective measurements on the self-other overlap

A mixed-design ANOVA with GROUP (stress and control) as between-participant factor and CONDITION (competition, cooperation and independent) as a within-participant factor was employed on the collected IOS scale. Results showed a significant main effect of CONDITION, $F(2, 172) = 22.12$, $P < 0.001$, $\eta_p^2 = 0.21$. A significant interaction effect of CONDITION × GROUP was also observed, $F(2, 172) = 4.44$, $P < 0.05$, $\eta_p^2 = 0.05$. The following simple effect analysis showed that the stress group's self-other overlap level during the cooperation session was significantly higher than that in the control group ($P < 0.05$). The results above were depicted in Figure 4.
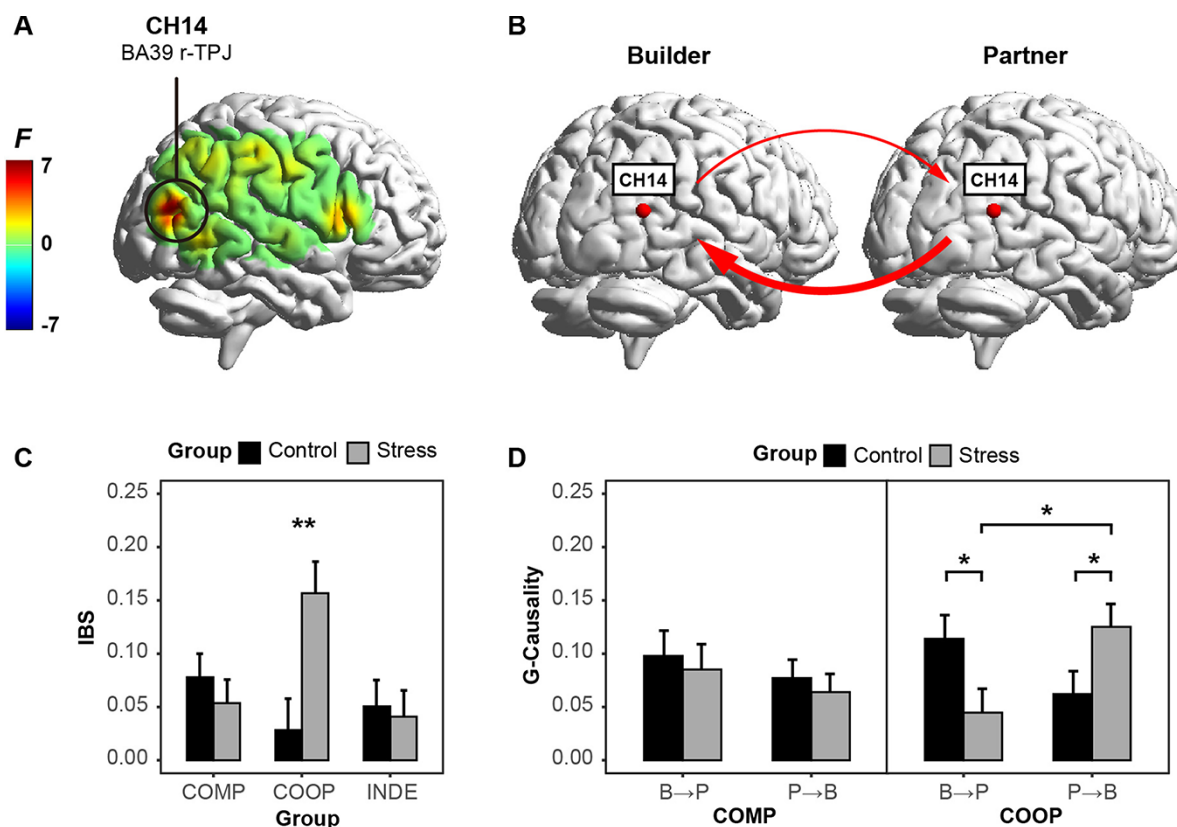
Fig. 5. Brain-to-brain coherence. (A) F-maps of IBS in the FOI; (B) Direction of IBS in CH14 (from BUILDER-to-PARTNER and PARTNER-to-BUILDER); (C) The mean IBS in all groups and all conditions; (D) The mean Granger causalities in two directions. Error bars represent standard errors of mean. * $P < 0.05$, ** $P < 0.01$.

Task-related interpersonal brain synchronization (IBS)

As mentioned above, a series of mixed-design ANOVAs using GROUP (stress and control) as between-participant factor and CONDITION (cooperation, competition and independent) as a within-participant factor were then conducted on tasked-related IBS of all channels. The yielded P-values were further corrected with the FDR correction method. Results only found a significant interaction effect of CONDITION × GROUP in the r-TPJ (i.e. CH14) in chosen FOI band, $F (2, 84) = 6.78$, FDR-corrected $P < 0.05$, $\eta_p^2 = 0.14$. The following simple effect analysis showed that the task-related IBS of the stress group was significantly higher than that of the control group during the cooperation session ($P < 0.01$). The results above were depicted in Figure 5.

Directional coupling

A mixed-design ANOVA with GROUP (stress and control) as a between-participant factor, CONDITION (cooperation, competition and independent) and DIRECTION (builder-to-partner and partner-to-builder) as within-participant factors were conducted on Granger causalities in CH14. Results found a significant interaction effect of CONDITION × GROUP × DIRECTION, $F (2, 84) = 4.02$, $P < 0.05$, $\eta_p^2 = 0.09$. The subsequent simple effect analysis showed that the G-causalities of the stress group was significantly lower than that of the control group during cooperation session in the builder-to-partner direction ($P < 0.05$), while G-causalities of the stress group were significantly higher than that of the control group during cooperation session in the partner-to-builder direction ($P < 0.05$). The G-causalities of the

partner-to-builder direction were also significantly higher than that of the builder-to-partner direction in the stress group during the cooperation session ($P < 0.05$).

Serial mediation model test

Before the serial mediation model test, the bivariate Pearson correlation analyses were conducted on the physiological, cognitive and neural results. The results were illustrated in Table 1.

As illustrated above, the correlations between the IBS and error rate during the competition session, as well as the correlation between the IOS and error rate during the competition session, were insignificant. Hence, we excluded the probability of
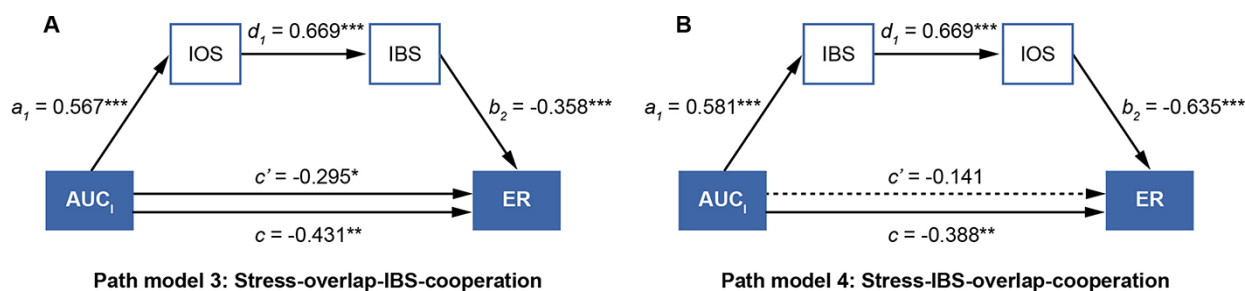
Table 1. Bivariate Pearson correlation results in the stress group

Variables	1	2	3	4	5	6	7
1 AUC$_I$	–	−0.181	−0.493*	0.226	0.567**	0.449*	0.581**
2 ER in COMP		–	−0.027	−0.253	−0.058	0.108	−0.107
3 ER in COOP			–	−0.077	−0.704*	−0.386	−0.519*
4 IOS in COMP				–	0.481*	−0.081	0.007
5 IOS in COOP					–	0.045	0.669*
6 IBS in COMP						–	0.143
7 IBS in COOP							–

*$P < 0.05$. **$P < 0.01$.

Fig. 6. Serial mediation analysis of IOS and IBS on the association between stress and cooperative performance. The dotted line represents the insignificant path coefficients. * $P < 0.05$, ** $P < 0.01$, *** $P < 0.001$.

Table 2. Fit indexes of the hypothesized path models

Path model	χ^2	df	RMSEA	CFI	TLI	SRMR
Path model 3	9.552	2	0.414	0.776	0.329	0.107
Path model 4	2.021	2	0.022	0.999	0.998	0.060

the hypothesized Path model 1 and Path model 2. Serial mediation analysis based on 1000 bootstrapping samples was further employed on Path model 3 and Path model 4. Results showed that the standardized total indirect effect of IOS and IBS on the relationship between acute stress and cooperative performance was −0.136, 95% CI = [−0.217, −0.071], while the standardized total indirect effect of IBS and IOS on the relationship between acute stress and cooperative performance was −0.247, 95% CI = [−0.378, −0.111]. The results above were depicted in Figure 6.

To further identify which path model was more fitted, the aforementioned fit indexes were calculated. The results were illustrated in Table 2. In line with prior studies, a path model was considered to be acceptable and reasonable when the aforementioned fit statistics above met the criteria below: $\chi^2/df < 3$, RMSEA < 0.08, SRMR < 0.10, CFI > 0.90, TLI > 0.90 (Kline, 2015; Arpaci and Baloğlu, 2016).

As illustrated above, the fit indexes of Path model 4 (stress—IBS—overlap-cooperation) met the criteria mentioned above in the prior studies, while the fit indexes of Path model 3 (stress—overlap—IBS—cooperation) exhibited a poor fit with the data in the present study. Hence, we identified Path model 4 (stress—IBS—overlap-cooperation) to be reasonable and acceptable.

Discussion

The current study has examined cognitive and neural mechanisms underlying the response pattern under acute stress in the turn-based interactive context by adopting the fNIRS-based hyperscanning technique. To our knowledge, the current research made the first attempt to uncover potential cognitive and neural mechanisms underlying the habitual response pattern under acute stress. Our results corroborated better performance in the cooperative context and further identified brain-to-brain coupling in r-TPJ and social connectedness coupling serially mediated the effect of acute stress on cooperative performance.

Better cooperative performance under acute stress

The present study investigated the females' habitual response patterns under acute stress in the real-time cooperative and competitive interaction context. During the cooperative session,

the error rate of the stress group was significantly lower than that of the control group, demonstrating better cooperative performance under acute stress. However, during the competitive session, the error rate of the stress group was significantly higher than that of the control group, indicating worse competitive performance under acute stress. Our results corroborated better cooperative performance during the cooperative session under acute stress and worse competitive performance during the competitive session under acute stress. Our results during the competitive session still aligned with several prior studies addressing lower competitive willingness and worse competitive performance under acute stress. Some prior studies also addressed that no significant impact of acute stress on competitive behavior was found (Zhong et al., 2018). We believed that this inconsistency among the existing research should be attributed to the more complicated factors underlying the competitive context under acute stress. On the one hand, the individuals' cognitive appraisal concerning the stressor may affect the competitive performance when facing the unexpected stressors under acute stress (Berger et al., 2016). On the other hand, individual differences in personality and behavioral style may also confuse the preferential response pattern under acute stress. Further studies are expected to further investigate how acute stress affects competitive interaction by considering the factors above.

Our results concerning the self-other overlap demonstrated that the self-other overlap level in the stress group during the cooperation session was significantly higher than that in the control group, demonstrating higher affiliative inclination of the stressed dyads during the cooperative session. The results above aligned with prior studies addressing that individuals' with higher salivary cortisol increased reported higher interpersonal closeness with the partner (Berger et al., 2016) and their wish for closeness (Von Dawans et al., 2019).

Brain-to-brain neural basis underlying the turn-based interaction under acute stress

At the brain-to-brain neural level, our results demonstrated that the task-related IBS of the stress group was significantly higher than that of the control group during the cooperative session, and the task-related IBS of the stress group during the cooperative session was also significantly higher than that during the competitive session. This task-related IBS increment of the stress group during the cooperative session was roughly mapped to the right AG (Brodmann Area 39), which was regarded as the main area in r-TPJ. As the core brain region in the MS (Wang et al., 2018), the r-TPJ was recruited in the mentalizing process (Wang et al., 2018), collaborative interaction (Tang et al., 2016), as well as theory of mind (Lu et al., 2020a). Recent hyperscanning studies also reported

that brain-to-brain coherence in r-TPJ could be associated with higher behavioral index of cooperative in the creativity tasks (Lu *et al.*, 2018), shared intentionality in the face-to-face interaction (Tang *et al.*, 2016), and joint attention interaction (Goelman *et al.*, 2019). In the present study, the increased task-related IBS in the stress group during the cooperative session was identified, and the IBS increment was correlated with higher self-other overlap levels and better cooperative performance. Our results further filled the theoretical vacancy on the neural mechanism underlying the social interaction under acute stress. We supposed that when the dyads completed that turn-based interactive game under acute stress during the cooperative session, the establishment and maintenance of coalitions and affiliations between the participants in the cooperative context has been promoted. This bonding and affiliation were manifested in higher subjective measurement levels on the degree of self-other overlap, which has been considered the core feature of social connectedness between individuals (Aron *et al.*, 1997). The significant correlation between the self-other overlap and the increased brain-to-brain coherence in r-TPJ also aligned with prior studies addressing that the brain-to-brain coupling can be the epiphenomenon of social connectedness in a shared social environment during social interaction (Dikker *et al.*, 2021; Gvirts and Perlmutter, 2020). The chain effect between the self-other overlap and brain-to-brain coherence was also examined, which was discussed in the following section.

Concerning the directionality of the brain-to-brain coherence, our results reported that BUILDER-to-PARTNER causality in the stress group during the cooperative session was significantly lower than that in the control group during the cooperative session, whereas PARTNER-to-BUILDER causality in the stress group during the cooperative session was significantly higher than that in the control group during the cooperative session. The PARTNER-to-BUILDER causality was also significantly stronger than the BUILDER-to-PARTNER causality of the stressed dyads in the cooperative context. Our results reported a reversing change of the coupling directionality in the cooperative context under acute stress. Specifically, the BUILDER-to-PARTNER directionality was stronger than the PARTNER-to-BUILDER directionality in the control group, while the BUILDER-to-PARTNER directionality was weaker than the PARTNER-to-BUILDER directionality in the stress group. We supposed that the reversing change under acute stress also aligned with the enhanced bonding and affiliation. When completing the cooperative task in the control group, the builder played the leading role in the interactive coordination, and the partner passively followed the builder's manipulations during the cooperative session. However, when completing the cooperative task in the stress group, the unexpected stressor promoted the bonding and alliance between the participants. The enhanced social connectedness between the builder and partner may contribute to the enhanced directionality from the partner to the builder.

Serial mediating effect: physiological—cognitive—neural—behavioral path model

By taking together the cognitive and neural mechanisms, we further tested the hypothesized four path models that we proposed in the introduction section. Our results corroborated Path model 4 (stress—IBS—overlap—cooperation), demonstrating that brain-to-brain coherence in r-TPJ and self-other overlap played a serial mediating role on how acute stress affected cooperative performance. We supposed that the enhancement of salivary

cortisol under acute stress preliminary acted on the brain-to-brain coherence. Increased neural coupling further promoted the social connectedness and affiliative bonding between participants under acute stress, and accordingly resulted in better cooperative performance. The present study aligned with the prior research addressing the serial mediating role that the self-other overlap and IBS played in social interaction (Feng *et al.*, 2020), and further filled the research vacancy on the cognitive and neural mechanism underlying the turn-based interaction under acute stress.

Limitations

The limitations in the current research should also be addressed. Firstly, the present study neglected the potential effect of the time delay on the turn-taking interaction when examining its underlying inter-brain correlates with the zero-lag approach due to the slow cerebral blood flow response and the current experimental design. Future studies with more sophisticated experimental design are expected to uncover the inter-brain connectivity pattern in the turn-taking interaction. Secondly, the individual variances within the dyad weren't taken into account when averaging into the dyad-level indexes. More delicate experimental design and method are expected to better manipulate the matching of participants on modeling the different dyad-level parameters. Thirdly, the difference in behavioral performance may also be caused by excessive cognitive load. Future studies are expected to examine the potential effect of the excessive cognitive load. At last, the mPFC which played an essential role in the self-other representation was not taken into consideration due to the characteristics of fNIRS devices. Future studies are expected to examine the inter-brain mechanism underlying the social interaction under acute stress with the neuroimaging technique with better spatial resolution, such as the fMRI-based hyperscanning technique.

Conclusions

The present study has made the first attempt to uncover the cognitive and neural mechanisms underlying the habitual response pattern in the turn-based interaction under acute stress. Our results corroborated better cooperative performance under acutes stress, and further identified that acute stress promoted the female dyads' cooperative performance via the chain effect of increased IBS in the r-TPJ and enhanced self-other overlap level.

Funding

Conflict of interest

None declared.

Supplementary data

Supplementary data are available at *SCAN* online.

References

Achard, S., Salvador, R., Whitcher, B., Suckling, J., Bullmore, E. (2006). A resilient, low-frequency, small-world human brain functional network with highly connected association cortical hubs. *Journal of Neuroscience*, **26**(1), 63–72.

Amodio, D.M., Frith, C.D. (2006). Meeting of minds: the medial frontal cortex and social cognition. *Nature Reviews Neuroscience*, **7**(4), 268–77.

Aron, A., Aron, E.N., Smollan, D. (1992). Inclusion of other in the self scale and the structure of interpersonal closeness. *Journal of Personality and Social Psychology*, **63**(4), 596.

Aron, A., Melinat, E., Aron, E.N., Vallone, R.D., Bator, R.J. (1997). The experimental generation of interpersonal closeness: a procedure and some preliminary findings. *Personality & Social Psychology Bulletin*, **23**(4), 363–77.

Arpaci, I., Baloğlu, M. (2016). The impact of cultural collectivism on knowledge sharing among information technology majoring undergraduates. *Computers in Human Behavior*, **56**, 65–71.

Berger, J., Heinrichs, M., von Dawans, B., Way, B.M., Chen, F.S. (2016). Cortisol modulates men's affiliative responses to acute social stress. *Psychoneuroendocrinology*, **63**, 1–9.

Bevilacqua, D., Davidesco, I., Wan, L., *et al.* (2019). Brain-to-brain synchrony and learning outcomes vary by student–teacher dynamics: evidence from a real-world classroom electroencephalography study. *Journal of Cognitive Neuroscience*, **31**(3), 401–11.

Blakemore, S.-J., Frith, C. (2003). Self-awareness and action. *Current Opinion in Neurobiology*, **13**(2), 219–24.

Booij, S.H., Bos, E.H., Bouwmans, M.E.J., *et al.* (2015). Cortisol and α-amylase secretion patterns between and within depressed and non-depressed individuals. *PLoS One*, **10**(7), e0131002.

Cannon, W.B. (1939). *The Wisdom of the Body*. New York: W.W. Norton & Company.

Chang, C., Glover, G.H. (2010). Time–frequency dynamics of resting-state brain connectivity measured with fMRI. *Neuroimage*, **50**(1), 81–98.

Chen, M., Zhang, T., Zhang, R., *et al.* (2020). Neural alignment during face-to-face spontaneous deception: does gender make a difference? *Human Brain Mapping*, **41**(17), 4964–81.

Cohen, J. (2013). *Statistical Power Analysis for the Behavioral Sciences*. New Jersey: Lawrence Erlbaum Associates.

Cohen, S. (2004). Social relationships and health. *American Psychologist*, **59**(8), 676.

Courtney, A.L., Meyer, M.L. (2020). Self-other representation in the social brain reflects social connection. *Journal of Neuroscience*, **40**(29), 5616–27.

Cui, X., Bryant, D.M., Reiss, A.L. (2012). NIRS-based hyperscanning reveals increased interpersonal coherence in superior frontal cortex during cooperation. *Neuroimage*, **59**(3), 2430–7.

De Dreu, C.K.W., Gross, J., Méder, Z., *et al.* (2016). In-group defense, out-group aggression, and coordination failures in intergroup conflict. *Proceedings of the National Academy of Sciences*, **113**(38), 10524.

Decety, J., Jackson, P.L., Sommerville, J.A., Chaminade, T., Meltzoff, A.N. (2004). The neural bases of cooperation and competition: an fMRI investigation. *Neuroimage*, **23**(2), 744–51.

Decety, J., Lamm, C. (2007). The role of the right temporoparietal junction in social interaction: how low-level computational processes contribute to meta-cognition. *The Neuroscientist*, **13**(6), 580–93.

Deutsch, M. (1973). *The Resolution of Conflict: Constructive and Destructive Processes*. New Haven: Yale University Press.

Dikker, S., Michalareas, G., Oostrik, M., *et al.* (2021). Crowdsourcing neuroscience: inter-brain coupling during face-to-face interactions outside the laboratory. *Neuroimage*, **227**, 117436.

Duan, H., Wang, X., Hu, W., Kounios, J. (2020). Effects of acute stress on divergent and convergent problem-solving. *Thinking & Reasoning*, **26**(1), 68–86.

Duan, H., Yang, T., Wang, X., *et al.* (2022). Is the creativity of lovers better? A behavioral and functional near-infrared spectroscopy hyperscanning study. *Current Psychology*, **41**(1), 41–54.

Dumas, G., Nadel, J., Soussignan, R., Martinerie, J., Garnero, L. (2010). Inter-brain synchronization during social interaction. *PLoS One*, **5**(8), e12166.

Eddy, C.M. (2016). The junction between self and other? Temporoparietal dysfunction in neuropsychiatry. *Neuropsychologia*, **89**, 465–77.

Faul, F., Erdfelder, E., Lang, A.-G., Buchner, A. (2007). G* Power 3: a flexible statistical power analysis program for the social, behavioral, and biomedical sciences. *Behavior Research Methods*, **39**(2), 175–91.

Feng, X., Sun, B., Chen, C., *et al.* (2020). Self–other overlap and interpersonal neural synchronization serially mediate the effect of behavioral synchronization on prosociality. *Social Cognitive and Affective Neuroscience*, **15**(2), 203–14.

Goelman, G., Dan, R., Stössel, G., Tost, H., Meyer-Lindenberg, A., Bilek, E. (2019). Bidirectional signal exchanges and their mechanisms during joint attention interaction–a hyperscanning fMRI study. *Neuroimage*, **198**, 242–54.

Granger, C.W.J. (1969). Investigating causal relations by econometric models and cross-spectral methods. *Econometrica*, **37**(3), 424–38.

Grinsted, A., Moore, J.C., Jevrejeva, S. (2004). Application of the cross wavelet transform and wavelet coherence to geophysical time series. *Nonlinear Processes in Geophysics*, **11**, 561–6.

Guijt, A.M., Sluiter, J.K., Frings-Dresen, M.H.W. (2007). Test-retest reliability of heart rate variability and respiration rate at rest and during light physical activity in normal subjects. *Archives of Medical Research*, **38**(1), 113–20.

Gvirts, H.Z., Perlmutter, R. (2020). What guides us to neurally and behaviorally align with anyone specific? A neurobiological model based on fNIRS hyperscanning studies. *The Neuroscientist*, **26**(2), 108–16.

Hasson, U., Ghazanfar, A.A., Galantucci, B., Garrod, S., Keysers, C. (2012). Brain-to-brain coupling: a mechanism for creating and sharing a social world. *Trends in Cognitive Sciences*, **16**(2), 114–21.

Hoshi, Y. (2003). Functional near-infrared optical imaging: utility and limitations in human brain mapping. *Psychophysiology*, **40**(4), 511–20.

Hu, Y., Hu, Y., Li, X., Pan, Y., Cheng, X. (2017). Brain-to-brain synchronization across two persons predicts mutual prosociality. *Social Cognitive and Affective Neuroscience*, **12**(12), 1835–44.

Igelström, K.M., Webb, T.W., Kelly, Y.T., Graziano, M.S.A. (2016). Topographical organization of attentional, social, and memory processes in the human temporoparietal cortex. *eNeuro*, **3**(2), 1–12. ENEURO.0060–0016.2016.

Izawa, S., Sugaya, N., Yamamoto, R., Ogawa, N., Nomura, S. (2010). The cortisol awakening response and autonomic nervous system activity during nocturnal and early morning periods. *Neuroendocrinology Letters*, **31**(5), 685.

Jiang, J., Dai, B., Peng, D., Zhu, C., Liu, L., Lu, C. (2012). Neural synchronization during face-to-face communication. *Journal of Neuroscience*, **32**(45), 16064–9.

Kan, Y., Duan, H., Chen, X., Wang, X., Xue, W., Hu, W. (2019). Attentional blink affected by acute stress in women: the role of affective stimuli and attentional resources. *Consciousness and Cognition*, **75**, 102796.

Keysers, C., Gazzola, V. (2007). Integrating simulation and theory of mind: from self to social cognition. *Trends in Cognitive Sciences*, **11**(5), 194–6.

Kline, R.B. (2015). *Principles and Practice of Structural Equation Modeling*. Guilford Publications. New York: Guilford publications.

Lieberman, M.D., Straccia, M.A., Meyer, M.L., Du, M., Tan, K.M. (2019). Social, self,(situational), and affective processes in medial prefrontal cortex (MPFC): causal, multivariate, and reverse inference evidence. *Neuroscience Biobehavioral Reviews*, **99**, 311–28.

Lindenberger, U., Li, S.-C., Gruber, W., Müller, V. (2009). Brains swinging in concert: cortical phase synchronization while playing guitar. *BMC Neuroscience*, **10**(1), 22.

Liu, T., Saito, H., Oi, M. (2015). Role of the right inferior frontal gyrus in turn-based cooperation and competition: a near-infrared spectroscopy study. *Brain and Cognition*, **99**, 17–23.

Liu, T., Saito, G., Lin, C., Saito, H. (2017). Inter-brain network underlying turn-based cooperation and competition: a hyperscanning study using near-infrared spectroscopy. *Scientific Reports*, **7**(1), 8684.

Lu, K., Xue, H., Nozawa, T., Hao, N. (2018). Cooperation makes a group be more creative. *Cerebral Cortex*, **29**(8), 3457–70.

Lu, K., Teng, J., Hao, N. (2020a). Gender of partner affects the interaction pattern during group creative idea generation. *Experimental Brain Research*, **238**(5), 1157–68.

Lu, K., Yu, T., Hao, N. (2020b). Creating while taking turns, the choice to unlocking group creative potential. *NeuroImage*, **219**, 117025.

Mahmoudzadeh, M., Dehaene-Lambertz, G., Fournier, M., *et al.* (2013). Syllabic discrimination in premature human infants prior to complete formation of cortical layers. *Proceedings of the National Academy of Sciences*, **110**(12), 4846.

Ménoret, M., Varnet, L., Fargier, R., *et al.* (2014). Neural correlates of non-verbal social interactions: a dual-EEG study. *Neuropsychologia*, **55**, 85–97.

Nozawa, T., Sasaki, Y., Sakaki, K., Yokoyama, R., Kawashima, R. (2016). Interpersonal frontopolar neural synchronization in group communication: an exploration toward fNIRS hyperscanning of natural interactions. *Neuroimage*, **133**, 484–97.

Oishi, S. (2000). *Goals Cornerstones of Subjective Well-Being Linking Individuals and Cultures Culture and Subjective Well-Being*. Cambridge, MA: MIT Press.

Osaka, N., Minamoto, T., Yaoi, K., Azuma, M., Osaka, M. (2014). Neural synchronization during cooperated humming: a hyperscanning study using fNIRS. *Procedia-Social and Behavioral Sciences*, **126**, 241–3.

Pan, Y., Cheng, X., Zhang, Z., Li, X., Hu, Y. (2017). Cooperation in lovers: an fNIRS-based hyperscanning study. *Human Brain Mapping*, **38**(2), 831–41.

Pan, Y., Dikker, S., Goldstein, P., Zhu, Y., Yang, C., Hu, Y. (2021). Instructor-learner brain coupling discriminates between instructional approaches and predicts learning. *Neuroimage*, **211**, 116657.

Pan, Y., Guyon, C., Borragán, G., Hu, Y., Peigneux, P. (2020). Interpersonal brain synchronization with instructor compensates for learner's sleep deprivation in interactive learning. *Biochemical Pharmacology*, **191**, 114111.

Pellicer, A., del Carmen Bravo, M. (2011). Near-infrared spectroscopy: a methodology-focused review. *Seminars in Fetal & Neonatal Medicine*, **16**(1), 42–9.

Pickering, M.J., Garrod, S. (2013). An integrated theory of language production and comprehension. *The Behavioral and Brain Sciences*, **36**(4), 329–47.

Pinti, P., Tachtsidis, I., Hamilton, A., *et al.* (2020). The present and future use of functional near-infrared spectroscopy (fNIRS) for cognitive neuroscience. *Annals of the New York Academy of Sciences*, **1464**(1), 5.

Pruessner, J.C., Kirschbaum, C., Meinlschmid, G., Hellhammer, D.H. (2003). Two formulas for computation of the area under the curve represent measures of total hormone concentration versus time-dependent change. *Psychoneuroendocrinology*, **28**(7), 916–31.

Reindl, V., Gerloff, C., Scharke, W., Konrad, K. (2018). Brain-to-brain synchrony in parent-child dyads and the relationship with emotion regulation revealed by fNIRS-based hyperscanning. *Neuroimage*, **178**, 493–502.

Salgues, S., Plancher, G., Jacquot, L., *et al.* (2021). To the self and beyond: arousal and functional connectivity of the temporo-parietal junction contributes to spontaneous sensations perception. *Behavioural Brain Research*, **396**, 112880.

Schroeter, M.L., Kupka, T., Mildner, T., Uludağ, K., von Cramon, D.Y. (2006). Investigating the post-stimulus undershoot of the BOLD signal—a simultaneous fMRI and fNIRS study. *Neuroimage*, **30**(2), 349–58.

Schweda, A., Faber, N.S., Crockett, M.J., Kalenscher, T. (2019). The effects of psychosocial stress on intergroup resource allocation. *Scientific Reports*, **9**(1), 18620.

Shields, G.S., Sazma, M.A., Yonelinas, A.P. (2016). The effects of acute stress on core executive functions: a meta-analysis and comparison with cortisol. *Neuroscience and Biobehavioral Reviews*, **68**, 651–68.

Smarr, K.L., Keefer, A.L. (2011). Measures of depression and depressive symptoms: beck depression inventory-II (BDI-II), center for epidemiologic studies depression scale (CES-D), geriatric depression scale (GDS), hospital anxiety and depression scale (HADS), and patient health Questionnaire-9 (PHQ-9). *Arthritis Care & Research*, **63**(S11), S454–66.

Starcke, K., Polzer, C., Wolf, O.T., Brand, M. (2011). Does stress alter everyday moral decision-making? *Psychoneuroendocrinology*, **36**(2), 210–9.

Steinbeis, N., Engert, V., Linz, R., Singer, T. (2015). The effects of stress and affiliation on social decision-making: investigating the tend-and-befriend pattern. *Psychoneuroendocrinology*, **62**, 138–48.

Takahashi, T. (2005). Social memory, social stress, and economic behaviors. *Brain Research Bulletin*, **67**(5), 398–402.

Tang, H., Mai, X., Wang, S., Zhu, C., Krueger, F., Liu, C. (2016). Interpersonal brain synchronization in the right temporo-parietal junction during face-to-face economic exchange. *Social Cognitive and Affective Neuroscience*, **11**(1), 23.

Taylor, S.E. (2006). Tend and befriend: biobehavioral bases of affiliation under stress. *Current Directions in Psychological Science*, **15**(6), 273–7.

Tomova, L., Majdandžić, J., Hummer, A., Windischberger, C., Heinrichs, M., Lamm, C. (2016). Increased neural responses to empathy for pain might explain how acute stress increases prosociality. *Social Cognitive and Affective Neuroscience*, **12**(3), 401–8.

Tong, Y., Lindsey, K.P., deB Frederick, B. (2011). Partitioning of physiological noise signals in the brain with concurrent near-infrared spectroscopy and fMRI. *Journal of Cerebral Blood Flow & Metabolism*, **31**(12), 2352–62.

Ulrich-Lai, Y.M., Herman, J.P. (2009). Neural regulation of endocrine and autonomic stress responses. *Nature Reviews Neuroscience*, **10**(6), 397–409.

Valencia, A.L., Froese, T. (2020). What binds us? Inter-brain neural synchronization and its implications for theories of human consciousness. *Neuroscience of Consciousness*, **2020**(1), niaa010.

Van Overwalle, F., Baetens, K. (2009). Understanding others' actions and goals by mirror and mentalizing systems: a meta-analysis. *Neuroimage*, **48**(3), 564–84.

Von Dawans, B., Kirschbaum, C., Heinrichs, M. (2011). The trier social stress test for groups (TSST-G): a new research tool for controlled simultaneous social stress exposure in a group format. *Psychoneuroendocrinology*, **36**(4), 514–22.

Von Dawans, B., Fischbacher, U., Kirschbaum, C., Fehr, E., Heinrichs, M. (2012). The social dimension of stress reactivity: acute stress increases prosocial behavior in humans. *Psychological Science*, **23**(6), 651–60.

Von Dawans, B., Ditzen, B., Trueg, A., Fischbacher, U., Heinrichs, M. (2019). Effects of acute stress on social behavior in women. *Psychoneuroendocrinology*, **99**, 137–44.

Wang, M., Luan, P., Zhang, J., Xiang, Y., Niu, H., Yuan, Z. (2018). Concurrent mapping of brain activation from multiple subjects during social interaction by hyperscanning: a mini-review. *Quantitative Imaging in Medicine and Surgery*, **8**(8), 819.

Wolf, O.T., Schulte, J.M., Drimalla, H., Hamacher-Dang, T.C., Knoch, D., Dziobek, I. (2015). Enhanced emotional empathy after psychosocial stress in young healthy men. *Stress*, **18**(6), 631–7.

Xia, M., Wang, J., He, Y. (2013). BrainNet viewer: a network visualization tool for human brain connectomics. *PLoS One*, **8**(7), e68910.

Xue, H., Lu, K., Hao, N. (2018). Cooperation makes two less-creative individuals turn into a highly-creative pair. *Neuroimage*, **172**, 527–37.

Yang, J., Zhang, H., Ni, J., De Dreu, C.K.W., Ma, Y. (2020). Within-group synchronization in the prefrontal cortex associates with intergroup conflict. *Nature Neuroscience*, **23**(6), 754–60.

Ye, J.C., Tak, S., Jang, K.E., Jung, J., Jang, J. (2009). NIRS-SPM: statistical parametric mapping for near-infrared spectroscopy. *Neuroimage*, **44**(2), 428–47.

Youssef, F.F., Dookeeram, K., Basdeo, V., *et al.* (2012). Stress alters personal moral decision making. *Psychoneuroendocrinology*, **37**(4), 491–8.

Zhang, H., Gross, J., De Dreu, C., Ma, Y. (2019). Oxytocin promotes coordinated out-group attack during intergroup conflict in humans. *Elife*, **8**, e40698.

Zhang, J., Liu, X., Ren, F., Sun, X., Yu, Q. (2016). The effects of group diversity and organizational support on group creativity. *Acta Psychologica Sinica*, **48**(12), 1551–60.

Zhang, M., Liu, T., Pelowski, M., Jia, H., Yu, D. (2017). Social risky decision-making reveals gender differences in the TPJ: a hyperscanning study using functional near-infrared spectroscopy. *Brain and Cognition*, **119**, 54–63.

Zhang, R., Zhou, X., Feng, D., *et al.* (2021). Effects of acute psychosocial stress on interpersonal cooperation and competition in young women. *Brain and Cognition*, **151**, 105738.

Zhao, H., Li, Y., Wang, Y., *et al.* (2021). Acute stress makes women's group decisions more rational: a functional near-infrared spectroscopy (fNIRS)–based hyperscanning study. *Journal of Neuroscience, Psychology, Economics*, **14**(1), 20.

Zheng, L., Liu, W., Long, Y., *et al.* (2020). Affiliative bonding between teachers and students through interpersonal synchronisation in brain activity. *Social Cognitive and Affective Neuroscience*, **15**(1), 97–109.

Zhong, S., Shalev, I., Koh, D., Ebstein, R.P., Chew, S.H. (2018). Competitiveness and stress. *International Economic Review*, **59**(3), 1263–81.

Zuo, X.-N., Di Martino, A., Kelly, C., *et al.* (2010). The oscillating brain: complex and reliable. *Neuroimage*, **49**(2), 1432–45.